

# Competitive Immunosorbent Assays Using Ligand–Enzyme Conjugates and Bifunctional Liposomes: Theory and Experiment

Matthew A. Jones, Peter K. Kilpatrick, and Ruben G. Carbonell\*

Department of Chemical Engineering, North Carolina State University, Raleigh, North Carolina 27695-7905

Two models of immuno-adsorbent assays are developed that describe the competitive adsorption of labeled antigen and unlabeled analyte to antibody binding sites immobilized on a solid surface. In the first model, a small labeled antigen and a small unlabeled analyte compete with only binding site limitations and no steric limitations. A multicomponent Langmuir isotherm results that is sufficient to quantify competitive adsorption. This model can describe, with no adjustable parameters, the data of competitive assays for biotin using biotinylated horseradish peroxidase (B-HRP) over a wide range of anti-biotin antibody (ABA) surface densities. In the second model, the small unlabeled analyte competes with a large colloidal particle containing many antigens and enzyme labels attached to its surface. This model quantifies the steric interference that large particles can experience upon binding (large ligand effect) due to the lower probability of finding an available area of the right size to accommodate the larger adsorbent. This large ligand model also takes into account the increased probability of binding a large particle due to the larger number of antibody binding sites covered per collision. The resulting model is used to analyze the competitive assay data of biotin competing with liposomes to which many biotin and HRP molecules have been conjugated. This analysis is of interest because previous work has shown that these bifunctional liposomes can reduce the detection limit for antigens in bulk solution relative to assays performed with conventional small labeled antigens.

## Introduction

In previous work (Jones et al., 1994), competitive immuno-adsorbent assays for the model antigen biotin were performed by using two different enzyme-labeled conjugates. In one method, small unilamellar phospholipid vesicles (liposomes) with covalently attached biotin and horseradish peroxidase (HBVs) were used as the labeled ligand. The results were compared to those obtained with commercially available biotin-labeled horseradish peroxidase (B-HRP) as the enzyme-labeled antigen. The antibody surface density on the microtiter plates was varied from monolayer coverage to about one-tenth of a monolayer (Jones et al., 1994). The lowest detectable antigen concentration (least detectable dose) for vesicles at low antibody surface density was found to be  $\sim 10^{-9}$  M, which is an order of magnitude lower than the value found using B-HRP ( $\sim 10^{-8}$  M). The assay sensitivity (slope of the response vs biotin concentration curve) using B-HRP was comparable to that using vesicles at a low antibody surface density. On the other hand, at high antibody loadings on the plate surface, the inhibition of HBV adsorption by free biotin was ineffective. It was postulated that the dependence on the antibody surface density of assays using vesicles was the result of multiple point attachment of vesicles to the surface (Jones et al., 1993, 1994).

In this paper, two models are developed to describe the behavior of each of the two types of competitive immuno-adsorbent assays. In the first model, a small analyte competes with a small labeled antigen for the antibody binding sites on the surface, with only binding site limitations and no steric limitations. This model will be referred to as the “small ligand model”. In the second

model, the small analyte competes with a large colloidal particle (such as a liposome) to which multiple antigens and labels are conjugated. If the particle diameter is greater than the distance between antibody binding sites on the surface, the particle adsorption is not limited by the available antibody binding sites. Instead, as more particles adsorb, there is a decreased probability that new particles will find a space that is sufficiently large to accommodate the particle within the available area not already covered by adsorbed particles. This has been called the “large ligand effect”, and models have been developed to calculate the adsorption probability for a particle as a function of the particle surface coverage (Schaaf and Talbot, 1989). At high antibody surface density, a large particle can cover several antibody binding sites. It is not unreasonable to imagine that this increases the probability of particle adsorption to the surface, since every time a particle collides it has several accessible antibody sites to which it can bind. This paper suggests a simple way of modeling this phenomenon, as well as the competition of a small ligand with a large particle for available surface sites. This second model will be referred to as the “large ligand model”.

The predictions of the small ligand model are compared to the results of competitive immuno-adsorbent assays using biotin as the small ligand and B-HRP as the labeled ligand. The association constants for biotin and B-HRP to ABA-coated surfaces have been measured independently (Jones et al., 1993). By using these values, the small ligand model can describe the competition behavior between biotin and B-HRP with no additional adjustable parameters. The large ligand model is used to analyze the competition data between biotin and HBVs over a wide range of antibody surface coverages. This model does an excellent job of describing all of the trends observed experimentally with the liposome-based immu-

\* Author to whom correspondence should be addressed.

**Table 1. Summary of Physical Parameters of Conjugates Used in Assays**

conjugate	diameter (Å)	biotin per conjugate <sup>a</sup>	HRP per conjugate <sup>a</sup>
B-HRP	60	1	1
[ <sup>14</sup> C]HBVs	890 ± 130	40	260
0.1 mol % HBVs	1480 ± 115	130	550

<sup>a</sup> Calculations based on average values (see Jones et al., 1994).

noadsorbent assays. The theory and experiments presented in this paper may also have applications to other problems involving molecular recognition steps between ligands bound to the surfaces of cells and viral particles.

### Materials and Methods

**Materials.** All materials were obtained as described in Jones et al. (1994).

**Methods.** The vesicles were prepared and characterized as described in Jones et al. (1994). Bifunctional vesicles with immobilized biotin and HRP were prepared with 0.1 mol % of total lipid containing immobilized biotin. The biotin was incorporated into the vesicles by coupling biotin to dimyristoylphosphatidylethanolamine (DMPE) through a coupling agent [as described in Jones et al. (1994)]. These vesicles are termed 0.1 mol % HBVs. Similar vesicles were prepared in which 10% of the added cholesterol (which comprised 37.5% of total lipid) was radiolabeled with <sup>14</sup>C. These vesicles are termed [<sup>14</sup>C]-HBVs, and the methods and procedures of preparing and characterizing the vesicles, performing the competitive immunoassays, and defining the parameters characterizing a particular assay are described in detail in Jones et al. (1993, 1994). The size and number of biotin and HRP molecules per conjugate for both the B-HRP and the bifunctional vesicles are provided in Table 1. Competitive assays to detect biotin were performed by using 0.1 mol % HBVs, B-HRP, and [<sup>14</sup>C]HBVs.

**Theoretical Model. Small Ligand Competitive Assay Model.** The small ligand competitive assay model (SLCAM), used for modeling labeled analyte at an equilibrium concentration [A\*] competing with unlabeled analyte, is based on the usual equilibrium binding reactions among labeled analyte, unlabeled analyte, and immobilized antibody. The competitive Langmuir model adequately describes the adsorption of labeled antigen in the presence of unlabeled analyte:

$$\frac{\Gamma_{A^*B}}{\Gamma_0} = \frac{K_2[A^*]}{1 + K_1[A] + K_2[A^*]} \quad (1)$$

In eq 1,  $\Gamma_{A^*B}$  and  $\Gamma_0$  are the surface concentration of labeled antigen bound to antibody and the surface density of total antibody active binding sites, respectively.  $K_1$  and  $K_2$  are the equilibrium binding constants, and [A] and [A\*] are the equilibrium bulk solution concentrations of unlabeled and labeled antigen, respectively. The association constants  $K_1$  and  $K_2$  can be determined by fitting the adsorption isotherms for the single components. The specific signals in a competitive assay depend on the surface concentration of labeled ligand,  $\Gamma_{A^*B}$ , at a given unlabeled analyte concentration [A]. The ratio of the signal obtained when the analyte concentration is [A] to that obtained when [A] = 0, at a fixed labeled analyte concentration [A\*], can be determined from eq 1:

$$\frac{S}{S_0} = \frac{1 + K_2[A^*]}{1 + K_1[A] + K_2[A^*]} \quad (2)$$

At equilibrium, the free labeled analyte concentration [A\*] is well approximated by the initial free analyte concentration [A\*]<sub>0</sub>, as only a very small percentage of the analyte inventory binds to the antibody that is adsorbed to the surface. Note that the ratio  $S/S_0$  approaches 1 when the analyte concentration [A] is small and approaches zero when the analyte concentration [A] is much greater than that of the labeled ligand concentration. The association constants in eq 2 are written with the implicit assumption that a single numerical value adequately represents the  $K$  value. In previous work (Jones et al., 1994), it was found that the association constant for B-HRP could be represented by a single association constant ( $K_2 = 2.72 \times 10^8 \text{ M}^{-1}$ ) obtained from the Langmuir equation. The best fit of the Langmuir model and the corresponding association constants of biotin, B-HRP, and HBVs binding to immobilized ABA are given in Table 2. Jones et al. (1994) also found that the binding of biotin to immobilized anti-biotin antibody was best described by assuming a distribution of association constants given by the Sips equation (Sips, 1948; Pauling et al., 1944; Nisonoff and Pressman, 1957), with an average value of the association constant of  $K_0 = 3.71 \times 10^7 \text{ M}^{-1}$  and a heterogeneity index of  $h = 0.82$ . As a result, a better model for the signals obtained in a competitive assay for biotin with immobilized anti-biotin can be derived by averaging eq 2 and using the distribution of association constants prescribed by the Sips equation:

$$\frac{\bar{S}}{S_0} = \int_0^\infty \frac{1 + K_2[A^*]}{1 + K_1[A] + K_2[A^*]} N(K_1) dK_1 \quad (3)$$

The differential distribution function for the number  $N(K)$  of binding sites with an association constant between  $K$  and  $K + dK$  is (Sips, 1948)

$$N(K) dK = \frac{-\sin(\pi h)(K/K_0)^h}{\pi K(1 + 2 \cos(\pi h)(K/K_0)^h + (K/K_0)^{2h})} dK \quad (4)$$

where

$$\int_0^\infty N(K) dK = 1 \quad (5)$$

The definite integral in eq 3 was evaluated numerically by using the IMSL subroutine QDAGS at fixed [A\*] values. These fixed values corresponded to the labeled analyte concentrations used in experimental competitive assays for [A] values ranging from  $10^{-13}$  to  $10^{-4}$  M biotin concentration. These results are discussed in the following section. Also,  $K_1$  and  $K_2$  values were varied to investigate the effects of the average association constant for unlabeled antigen and the association constant for labeled antigen on the competitive assay performance as predicted by the SLCAM. The SLCAM results from eq 3 are also compared to the experimental assay results of  $S/S_0$  that follow.

**Large Ligand Competitive Assay Model.** The competitive assay model developed here for biotin-conjugated vesicles competing with free biotin in solution is called the large ligand competitive assay model (LLCAM). In the development here, biotin is the unlabeled antigen, designated by subscript 1, and HBVs are the labeled antigen, designated by subscript 3. In developing the LLCAM, it is assumed that the binding rate of unlabeled antigen is proportional to the free active antibody sites  $\Gamma_0 - \Gamma_{AB}$  and that the area covered by the vesicles is not

**Table 2. Association Constants of Biotin, B-HRP, and HBVs with Surface-Adsorbed ABA**

species	total ABA surface density (ng/cm <sup>2</sup> )	Langmuir $K^a$ (nm <sup>-1</sup> )	Sips $K^b$ (nM <sup>-1</sup> )	heterogeneity index, $h$	large ligand model $K^c$ (nM <sup>-1</sup> )
[ <sup>14</sup> C]biotin	290	0.072	0.037	0.82	NA <sup>d</sup>
B-HRP	290	0.27	0.29	1.0	NA
[ <sup>14</sup> C]HBVs	290	2.0	2.5	1.3	0.3
	79	1.5	1.7	1.0	0.4

<sup>a</sup>  $K$  determined from the Langmuir model (eq 2). <sup>b</sup>  $K$  determined from the Sips model (eq 3). <sup>c</sup>  $K$  determined from the large ligand model (eq 10). <sup>d</sup> NA, not applicable.

available to unlabeled antigen. The fraction of microtiter well surface area occupied by vesicles is  $\theta$ . The net rate of adsorption of unlabeled antigen (biotin) can then be written in the form

$$R_A = \frac{d\Gamma_A}{dt} = k_1(1 - \theta)(\Gamma_0 - \Gamma_{AB})[A] - k_{-1}\Gamma_{AB} \quad (6)$$

The probability of a large ligand, such as a vesicle, finding an area large enough to allow adsorption is designated  $P(\theta)$  and is given by Schaaf and Talbot (1989) as

$$P(\theta) = \exp\left\{2 - \frac{2}{(1 - \theta)^2} + \frac{7\theta}{8(1 - \theta)^2} + \frac{7}{8}\ln(1 - \theta)\right\} \quad (7)$$

When the active antibody surface density is low enough that multiple point attachment is unlikely, the probability of the large ligand finding a vacant active antibody binding site is proportional to the fraction of free antibody sites,  $1 - \Gamma_{AB}/\Gamma_0$ . As the antibody surface density increases, the probability of the large ligand finding vacant binding sites increases. The reason for this is that a large ligand will cover many antibodies as it approaches the surface. It is expected that the smaller the ratio of the vesicle cross-sectional area to the area occupied per adsorbed antibody molecule, the larger the rate of vesicle adsorption. The probability of a large ligand finding vacant antibody binding sites and adsorbing can then be written as  $(1 - \Gamma_{AB}/\Gamma_0)^m$ , where  $m$  should be proportional to the area per active site divided by the area per vesicle ( $A/A_0$ ) where  $A < A_0$ . Therefore, the parameter  $m$  can take on a value between 0 and 1. When the antibody surface density is high,  $m$  should be small, while  $m$  should approach 1 when the antibody surface density is low enough to result in one-to-one binding. The net rate of vesicle adsorption can then be written as

$$R_{A^*} = \frac{d\Gamma_{A^*}}{dt} = k_3P(\theta)(1 - \Gamma_{AB}/\Gamma_0)^m[A^*] - k_{-3}\theta \quad (8)$$

By setting eq 8 equal to zero and solving for  $\theta$ , we obtain

$$\theta = K_3(1 - \Gamma_{AB}/\Gamma_0)^mP(\theta)[A^*] \quad (9)$$

where  $K_3$  is the equilibrium binding constant of liposomes to antibody on the surface. It must be kept in mind that  $K_3$  is an effective binding constant characterizing the interaction of immobilized biotin on the vesicular surface with immobilized antibody on the microtiter well surface. It is calculated on the basis of the molar concentration of the interacting species (vesicles) rather than immobilized biotin because only a fraction of the immobilized biotin will be accessible to the surface. By setting eq 6 equal to zero, solving for  $1 - \Gamma_{AB}/\Gamma_0$ , and substituting the resulting expression into eq 9, we obtain

$$\theta = \frac{K_3P(\theta)[A^*]}{(1 + K_1(1 - \theta)[A])^m} \quad (10)$$

In deriving eq 10, we assumed that  $[A^*] \approx [A^*]_0$ , which is an excellent assumption because the amount of labeled analyte adsorbed to the surface is a very small percentage of the total labeled analyte. This is the equation for the fraction of the surface covered by vesicles in competition with small ligands (analyte) in solution. By allowing the concentration of unlabeled antigen  $[A]$  to approach zero in eq 10, we obtain an expression for the surface coverage of liposomes in the absence of free analyte:

$$\theta_0 = K_3[A^*]P(\theta_0) \quad (11)$$

This is the large ligand isotherm for vesicles (Jones et al., 1994), and it can be used to calculate  $K_3$  values by fitting experimental data for vesicle adsorption in the absence of small ligand. The signal  $S$  obtained at a given analyte concentration divided by the maximum signal  $S_0$  determined when  $[A] = 0$  is proportional to the ratio  $\theta/\theta_0$ . The results of determining  $m$  values by nonlinear least-squares regression of eq 10 by using experimental values for  $K_3$  ( $1 \times 10^9 \text{ M}^{-1}$ ) and  $K_1$  ( $7.25 \times 10^7 \text{ M}^{-1}$ ) are discussed in the following section. The effect of antibody heterogeneity was not accounted for in this calculation, and the  $K_1$  value from the Langmuir isotherm model was used for unlabeled antigen. The LLCAM (eq 10) was evaluated at fixed  $[A^*]$  values used in experimental competitive assays at  $[A]$  values ranging from  $10^{-13}$  to  $10^{-4}$  M biotin concentration. Also,  $K_1$  and  $K_3$  values were varied to investigate the effects of the average association constant for antigen and the association constant for vesicles on the competitive assay performance as predicted by the LLCAM. The large ligand competitive assay model results for the average  $\theta/\theta_0$  are also compared to experimental assay results of  $S/S_0$ . These results are described in the following section.

## Results and Discussion

The physical parameters of the enzyme-labeled conjugates used in competitive assays are listed in Table 1. Commercially available B-HRP had approximately one biotin molecule per enzyme according to the manufacturer (Sigma). The diameter of HRP, estimated from sedimentation velocity measurements (Cecil and Ogston, 1951; Jones et al., 1993) as 60 Å, was taken to be equal to the diameter of B-HRP. The vesicle physical parameters, determined in previous work (Jones et al., 1994), are also listed in Table 1. For [<sup>14</sup>C]HBVs, the average diameter was 890 Å, and there were approximately 260 HRP molecules and 40 biotin molecules on the vesicle surface. For 0.1 mol % HBVs, the average diameter was 1480 Å, and there were approximately 550 HRP molecules and 130 biotin molecules on the vesicle surface. Both vesicle preparations contained 0.1 mol % biotin-labeled phospholipid, but the number of biotin molecules per vesicle was greater for 0.1 mol % HBVs because of their larger size.

The determination of association constants for [ $^{14}\text{C}$ ]biotin, B-HRP, and [ $^{14}\text{C}$ ]HBVs from adsorption isotherms was described in previous work (Jones et al., 1994). Association constants for [ $^{14}\text{C}$ ]biotin and B-HRP were determined from the Langmuir equation and the Sips equation, while association constants for [ $^{14}\text{C}$ ]HBVs were determined from the Langmuir equation, the Sips equation, and the large ligand equation. The association constants are summarized in Table 2. The adsorption isotherms of [ $^{14}\text{C}$ ]biotin and B-HRP were performed by using microtiter wells coated with 290 ng/cm<sup>2</sup> antibody, while the vesicle isotherms were performed at antibody surface densities of 290 and 79 ng/cm<sup>2</sup>. The association constant for [ $^{14}\text{C}$ ]biotin was about an order of magnitude smaller than the association constant for B-HRP and about 2 orders of magnitude smaller than the association constant for [ $^{14}\text{C}$ ]HBVs. This indicates that the binding was strongest for vesicles, followed by B-HRP and free biotin. The enhanced binding constant of B-HRP relative to [ $^{14}\text{C}$ ]biotin is undoubtedly due to additional attractive forces (electrostatic, hydrogen bonding, van der Waals, or hydrophobic) between the antibody and B-HRP. With the [ $^{14}\text{C}$ ]HBVs, the situation is a bit more complex. The vesicles have, on average, 40 immobilized biotin molecules and thus would be expected to have a proportionately higher binding constant. However, once one biotin moiety binds to the surface, the majority of the remaining biotin moieties have no access to bind due to the lack of deformability of the small vesicles. Undoubtedly, the enhanced binding constant of vesicles for the surface is due in part to multiple binding of biotins and may be due to some additional secondary forces of attraction (van der Waals, hydrophobic, etc.) between the vesicles and the surface. It is also possible that the enhancement in binding constant of the B-HRP conjugate and the HBVs, relative to free biotin, may in part be attributed to the fact that the polyclonal antibodies to which these labeled antigens are binding were developed against biotin immobilized as a hapten on a proteinaceous antigen, and antibody may have some affinity for the bridging link between hapten and protein. Precise deduction of the origin of the enhanced affinity of biotin conjugate relative to free biotin is beyond the scope of this paper.

As indicated by the values for the heterogeneity index in Table 2, the heterogeneity of antibody binding sites was found to be greatest for [ $^{14}\text{C}$ ]biotin, while little or no binding site heterogeneity was found for B-HRP and [ $^{14}\text{C}$ ]HBVs. The absence of antibody heterogeneity for B-HRP and [ $^{14}\text{C}$ ]HBVs probably results from the biotin moiety being covalently attached to the conjugate and therefore restricted in its possible binding orientations. Free biotin, on the other hand, has no such restrictions. According to Sips (1948) the maximum heterogeneity index is 1, so that the  $h$  value of 1.3 found for vesicles at 290 ng/cm<sup>2</sup> theoretically is not possible. It is likely that this anomalous value is a result of multiple point attachment of vesicles to the antibody-coated surface (Jones et al., 1994) or a forced fit of the model in an instance in which it may not be expected to apply. It should be noted that the association constant for vesicles determined from a given adsorption isotherm model is not very sensitive to the antibody surface density. For example, when the antibody surface density was increased by a factor of nearly 4, the association constant from the Langmuir equation or the large ligand model was essentially unchanged. These results indicate that the number of antibody binding sites on the well surface bound to an adsorbed vesicle does not affect the magnitude of the association constant. This suggests that only a few antibody binding sites are required for vesicle

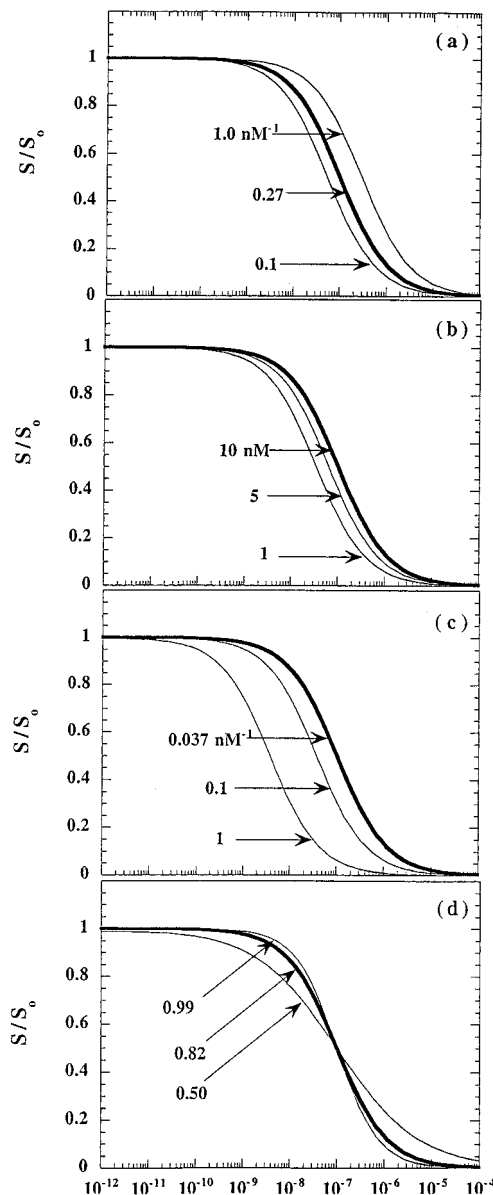


**Figure 1.** Predictions of the small ligand competitive assay model (SLCAM, eq 3): effects of varying the association constant of labeled ligand  $K_2$ , the labeled ligand concentration  $[A^*]$ , average association constant of unlabeled ligand  $K_1$ , and the Sips heterogeneity index  $h$  on the response  $S/S_0$ . Panel a:  $K_2 = 1 \times 10^9$ ,  $2.72 \times 10^8$ , and  $1 \times 10^8 \text{ M}^{-1}$ ,  $K_0 = 3.71 \times 10^7 \text{ M}^{-1}$ ,  $h = 0.82$ , and  $[A^*] = 10 \text{ nM}$ . Panel b:  $[A^*] = 1-10 \text{ nM}$ ,  $K_1 = 3.71 \times 10^7 \text{ M}^{-1}$ ,  $h = 0.82$ , and  $K_2 = 2.72 \times 10^8 \text{ M}^{-1}$ . Panel c:  $K_1 = 3.71 \times 10^7$ ,  $1 \times 10^8$ , and  $1 \times 10^9 \text{ M}^{-1}$ ,  $K_2 = 2.72 \times 10^8 \text{ M}^{-1}$ ,  $h = 0.82$ , and  $[A^*] = 10 \text{ nM}$ . Panel d:  $h = 0.50-0.99$ ,  $K_1 = 3.71 \times 10^7 \text{ M}^{-1}$ ,  $K_2 = 2.72 \times 10^8 \text{ M}^{-1}$ , and  $[A^*] = 10 \text{ nM}$ .

adsorption, and above some threshold site density, additional sites do not promote stronger binding. This aspect of vesicle adsorption is discussed in more detail later when comparing experimental assay results with the competitive assay model.

**Small Ligand Competitive Assay Model—Computer Simulations.** The immunoassay models developed in the Theoretical Model section, represented by eqs 3 and 10, were studied parametrically to determine their intrinsic sensitivity to the variation of equilibrium binding constants  $K_1$  and  $K_2$ , Sips heterogeneity index  $h$ , labeled ligand concentration  $[A^*]$ , and cooperativity parameter  $m$ . The results of this parametric study with the SLCAM are shown in Figure 1, in which  $K_2$ ,  $[A^*]$ ,  $K_1$ , and  $h$  were varied to determine their effect on the assay response  $S/S_0$  (eq 3) on unlabeled antigen concen-

trations ranging from  $10^{-12}$  to  $10^{-4}$  M. It was found in previous work that the experimental value of  $K_2$  was  $2.72 \times 10^8 \text{ M}^{-1}$ ,  $K_1$  was  $3.71 \times 10^7 \text{ M}^{-1}$ ,  $h$  was 0.82, and the range of  $[A^*]$  in competitive assays was 1–10 nM (Jones et al., 1994). These values, with an  $[A^*]$  of 10 nM, are represented by the bold line in parts a–d of Figure 1. In part a, the association constant for labeled ligand  $K_2$  is varied from 0.1 to 1.0  $\text{nM}^{-1}$ . As the  $K_2$  value decreases, the competitive assay curves shift to slightly lower free antigen concentrations. This lowers the least detectable dose (LDD) and the half-maximal dose (HMD), while the slope of the response (SR) is not changed significantly.

The labeled ligand concentration  $[A^*]$  is varied from 1 to 10 nM on the response  $S/S_0$ , with resulting predictions shown in part b of Figure 1. As the  $[A^*]$  value is decreased over this range, the LDD and HMD values are lowered slightly and the SR is not changed significantly.

The association constant for unlabeled ligand  $K_1$  has a much more dramatic effect on the response  $S/S_0$ , as shown in Figure 1c in which  $K_1$  is varied from 0.037 to 1.0  $\text{nM}^{-1}$ . Here, the response curves are shifted by an order of magnitude to lower free antigen concentrations. Accordingly, the LDD and HMD values decrease as the  $K_1$  value increases, indicating that lower detection limits are possible when the association constant of the unlabeled ligand increases. The  $K_1$  value is directly influenced by the affinity of the antibody for unlabeled antigen. This result indicates that if the antibody affinity can be increased for the analyte, the lower detection limit of the assay can be improved significantly.

The effect of varying the antibody heterogeneity index  $h$  from 0.99 to 0.5 on the response  $S/S_0$  as predicted by the SLCAM is shown in Figure 1d. As the  $h$  value decreases the SR becomes less negative, indicating a loss of sensitivity. The LDD value is lowered slightly, and the HMD value remains unchanged. This result indicates that the competitive assay sensitivity could be improved by using a monoclonal antibody, whose binding affinity can be characterized by a single association constant (Goding, 1983).

**Large Ligand Competitive Assay Model—Computer Simulations.** The values of  $K_3$ ,  $[A^*]$ ,  $K_1$ , and  $m$  were varied to determine the qualitative effect on the assay response  $S/S_0$  as predicted by the large ligand competitive assay model (LLCAM, eqs 10 and 11) at unlabeled antigen concentrations ranging from  $10^{-12}$  to  $10^{-4}$  M. The results of computer simulations using the LLCAM are shown in Figure 2a–d. It was found from prior experimental work with biotin as the ligand that the value of  $K_3$  was between 0.1 and 1.0  $\text{nM}^{-1}$ ,  $K_1$  was  $7.25 \times 10^7 \text{ M}^{-1}$ , and the range of  $[A^*]$  in competitive assays was 20.5–113 pM (Jones et al., 1994). The bold lines in Figure 2 represent solutions for a value of  $K_3$  of 1  $\text{nM}^{-1}$ , a value of  $K_1$  of 0.0725  $\text{nM}^{-1}$ ,  $m = 1.0$ , and an  $[A^*]$  value of 0.1 nM.

The effect of varying the association constant for labeled ligand  $K_3$  from 0.1 to 10  $\text{nM}^{-1}$  on the response  $S/S_0$  is shown in Figure 2a. The labeled ligand concentration  $[A^*]$  is varied from 1 to 0.01 nM and the results are shown in Figure 2b. The predicted assay response was only modestly affected by these two variables. The effect of varying the association constant for unlabeled ligand  $K_1$  from  $1 \times 10^6$  to  $1 \times 10^9 \text{ M}^{-1}$  is shown in Figure 2c. The response curves are shifted by several orders of magnitude to lower ligand concentrations as  $K_1$  is increased. Accordingly, the LDD and HMD values decrease as the  $K_1$  value decreases, indicating that lower detection limits are possible when the association constant of the unlabeled ligand increases. These findings are similar

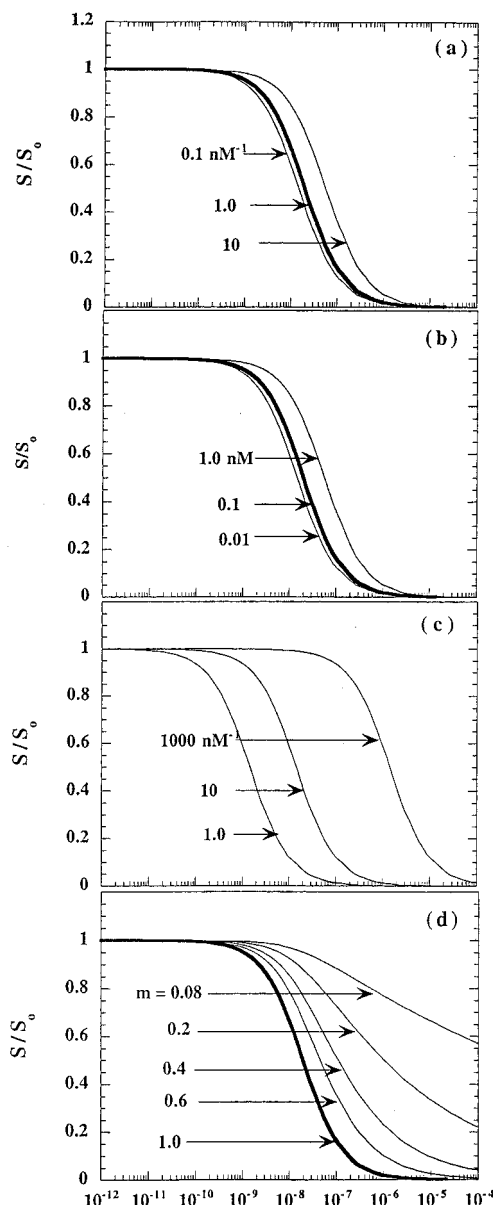


**Figure 2.** Predictions of the large ligand competitive assay model (LLCAM, eqs 10 and 11): effects of varying the association constant of labeled ligand  $K_3$ , the labeled ligand concentration  $[A^*]$ , the average association constant of unlabeled ligand  $K_1$ , and the cooperativity parameter  $m$  on the response  $S/S_0$ . Panel a:  $K_3 = 1 \times 10^8$ ,  $1 \times 10^9$ , and  $1 \times 10^{10} \text{ M}^{-1}$ ,  $K_1 = 7.25 \times 10^7 \text{ M}^{-1}$ ,  $m = 1.0$  and  $[A^*] = 0.1 \text{ nM}$ . Panel b:  $[A^*] = 1, 0.1,$  and  $0.01 \text{ nM}$ ,  $K_1 = 7.25 \times 10^7 \text{ M}^{-1}$ ,  $m = 1.0$ , and  $K_3 = 1 \times 10^9 \text{ M}^{-1}$ . Panel c:  $K_1 = 1 \times 10^6, 1 \times 10^8,$  and  $1 \times 10^9 \text{ M}^{-1}$ ,  $K_3 = 1 \times 10^9 \text{ M}^{-1}$ ,  $m = 1.0$ , and  $[A^*] = 0.1 \text{ nM}$ . Panel d:  $m = 1.0, 0.60, 0.40, 0.20,$  and  $0.08$ ,  $K_1$  value was  $7.25 \times 10^7 \text{ M}^{-1}$ ,  $K_3 = 1 \times 10^9 \text{ M}^{-1}$ , and  $[A^*] = 0.1 \text{ nM}$ .

to the results found for the SLCAM when  $K_1$  was changed as discussed earlier.

The effect of varying  $m$  from 1.0 to 0.08 on the response  $S/S_0$  is shown in Figure 2d. As the  $m$  value increases, the slope of the response curve becomes more negative, indicating better sensitivity, while the LDD and the HMD values also decrease. This is because as the  $m$  value increases, the probability of the large ligand finding an available binding site decreases. On the other hand, as the probability of the large ligand finding an available binding site increases, the large ligand dominates the adsorption process and the competitive assay becomes less effective. As noted earlier,  $m$  should be proportional to the area ratio of binding site to vesicle ( $A/A_0$ ). For a given vesicle diameter,  $A_0$  is fixed, so that as the antibody

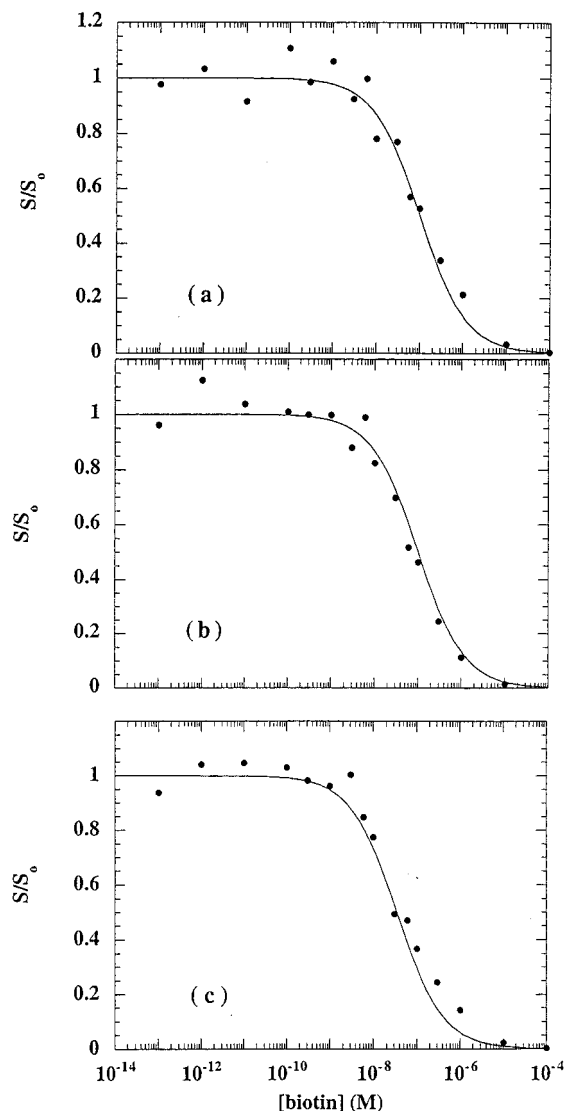


**Figure 3.** Comparison of experimental competitive assay data (circles) with the SLCAM (solid lines):  $K_2 = 2.72 \times 10^8 \text{ M}^{-1}$ ,  $K_1 = 3.71 \times 10^7 \text{ M}^{-1}$ , and the  $h = 0.82$ . (a) The antibody surface density was  $250 \text{ ng/cm}^2$  and the B-HRP concentration was  $10 \text{ nM}$ . (b) The antibody surface density was  $33 \text{ ng/cm}^2$  and the B-HRP concentration was  $10 \text{ nM}$ . (c) The antibody surface density was  $250 \text{ ng/cm}^2$  and the B-HRP concentration was  $1 \text{ nM}$ .

surface density increases,  $A/A_0$  decreases. Thus,  $m$  should decrease as the antibody surface density increases. Experimental  $m$  values are compared with theoretical  $A/A_0$  values later.

**Small Ligand Competitive Assay Model Results—Comparison with Experiment.** Representative experimental assay results using B-HRP are compared with the SLCAM in Figure 3, in which the response ( $S/S_0$ ) is plotted as a function of the biotin concentration. The models (solid lines) were calculated at the noted labeled ligand concentration described earlier. The  $K_2$  value was  $2.72 \times 10^8 \text{ M}^{-1}$ , the  $K_1$  value was  $3.71 \times 10^7 \text{ M}^{-1}$ , and the  $h$  value was  $0.82$ , which were all obtained from independent experiments. In Figure 3a the ABA surface density was  $290 \text{ ng/cm}^2$ . This corresponds to a bulk concentration of adsorbing ABA of  $10 \mu\text{g/mL}$  (Jones et al., 1994). The B-HRP concentration in Figure 3a was  $1 \times 10^{-8} \text{ M}$ . These conditions are the maximum antibody surface density and B-HRP concentration used in the assays. In Figure 3b the ABA surface density was  $38 \text{ ng/cm}^2$ , corresponding to a bulk concentration of adsorbing ABA of  $0.5 \mu\text{g/mL}$ . This was the minimum ABA

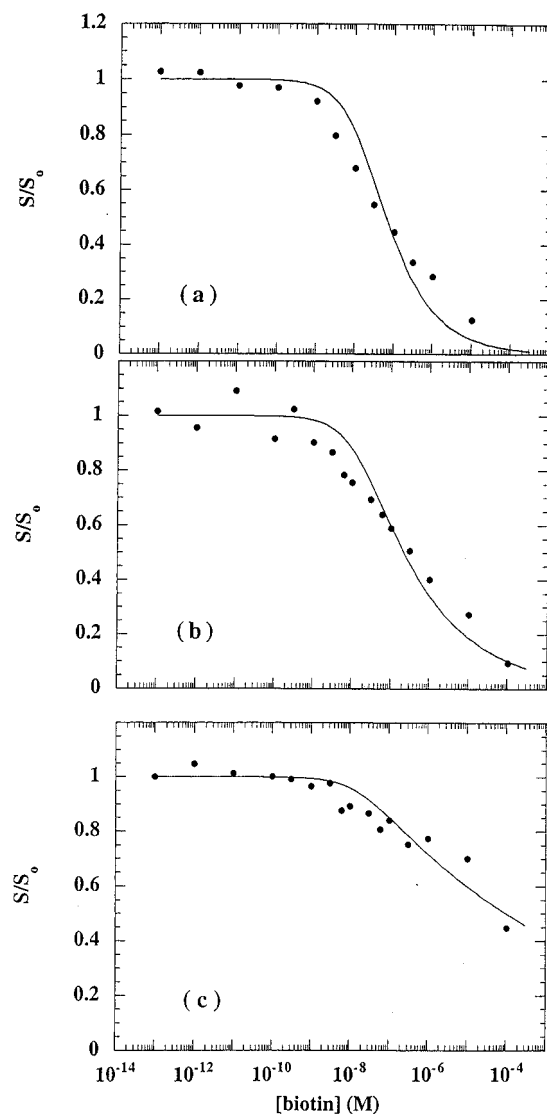


**Figure 4.** Comparison of experimental competitive assay data (circles) with the LLCAM (solid lines):  $K_3 = 1 \times 10^9 \text{ M}^{-1}$  and  $K_1 = 7.25 \times 10^7 \text{ M}^{-1}$ . (a) The antibody surface density was  $59 \text{ ng/cm}^2$ , the  $[^{14}\text{C}]\text{HBV}$  concentration was  $5.65 \times 10^{-11} \text{ M}$ , and  $m = 0.48$ . (b) The antibody surface density was  $156 \text{ ng/cm}^2$ , the  $0.1 \text{ mol \% HBV}$  concentration was  $3.07 \times 10^{-11} \text{ M}$ , and  $m = 0.27$ . (c) The antibody surface density was  $290 \text{ ng/cm}^2$ , the  $0.1 \text{ mol \% HBV}$  concentration was  $2.05 \times 10^{-11} \text{ M}$ , and  $m = 0.083$ .

surface density examined. The B-HRP concentration in Figure 3b was  $1 \times 10^{-8} \text{ M}$ . In Figure 3c the ABA surface density was  $250 \text{ ng/cm}^2$  and the B-HRP concentration was  $1 \times 10^{-9} \text{ M}$ , which was the minimum B-HRP concentration used. The model fits the experimental data adequately with no adjustable parameters throughout the entire range of biotin concentrations in the three plots shown in Figure 3. Similar results were found for other assays using B-HRP as marker-labeled antigen (Jones, 1993).

**Large Ligand Competitive Assay Model Results—Comparison with Experiment.** Two separate batches of liposomes with both HRP and biotin conjugated to them ( $0.1 \text{ mol \% HBVs}$  and  $[^{14}\text{C}]\text{HBVs}$ ) were prepared and used in competitive assays. Representative experimental assay results using HBVs are compared with the LLCAM in Figure 4, in which the response ( $S/S_0$ ) is plotted as a function of the biotin concentration. The model predictions (solid lines) were obtained by fitting  $m$  using nonlinear least-squares regression from eq 10 with a  $K_3$  value of  $1 \text{ nM}^{-1}$  and a  $K_1$  value of  $0.0725 \text{ nM}^{-1}$ .

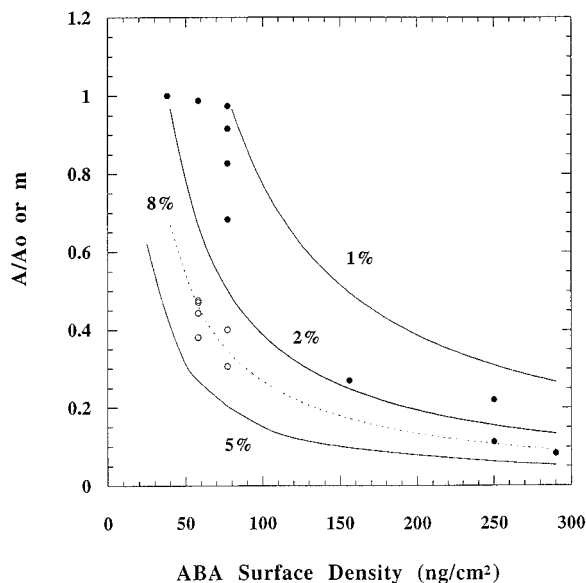


**Figure 5.** Comparison of theoretical  $A/A_0$  values to experimental  $m$  values for vesicles with two different mean diameters: (a) 0.1 mol % HBVs (diameter = 1480 Å) with lines for  $A/A_0$  of 5%, 2%, and 1%; (b) [ $^{14}\text{C}$ ]HBVs (diameter = 890 Å) with  $A/A_0$  of 8%.

In Figure 4a, the antibody surface density was 59 ng/cm<sup>2</sup> and the  $m$  value was 0.48. In Figure 4b, the antibody surface density was 156 ng/cm<sup>2</sup> and the  $m$  value was 0.27. In Figure 4c, the antibody surface density was 290 ng/cm<sup>2</sup> and the  $m$  value was 0.083. It is clear that the  $m$  values decrease as the antibody surface density increases. This is because the probability of vesicle adsorption increases with increasing binding site surface density. As a result, competitive assays with large ligand are less effective at high than at low antibody site density. This suggests that only a few surface binding sites per adsorbing vesicle may be required for effective vesicle adsorption. When there are more than a few binding sites per adsorbing vesicle in competitive assays, the extra sites could be occupied by antigen, yet fail to inhibit vesicle binding. Under these conditions, the free antigen concentration would have to be increased dramatically to affect the vesicle adsorption. The notion that only a few antibody binding sites are required for vesicle adsorption is supported by the fact that the association constant was unaffected by the antibody surface density between monolayer coverage and one-tenth of a monolayer (Jones et al., 1993, 1994).

As noted earlier,  $m$  is expected to be proportional to the ratio of the area per active antibody binding site and the projected area of the vesicle ( $A/A_0$ ). The theoretical ratio can be estimated from the active antibody surface density and the vesicle diameter. In work performed before the optimization of plate-coating conditions, determinations of adsorbed B-HRP indicated that the antibody activity decreases as the total antibody surface coverage decreases (Jones et al., 1993). As the antibody surface density decreases, the extent of hydrophobic interaction between adsorbed antibody molecules and the polystyrene microtiter plate surface is likely to increase and cause the decrease in antibody activity. By using optimized plate-coating conditions and radiolabeled biotin, it was found that microtiter plate wells coated with 290 ng/cm<sup>2</sup> antibody resulted in  $4.3 \times 10^{11}$  sites/cm<sup>2</sup> and the ABA was approximately 20% active (Jones et al., 1994). From these results, the adsorbed antibody activity is expected to decrease from 20% at 290 ng/cm<sup>2</sup> total antibody to approximately 1% at low antibody surface

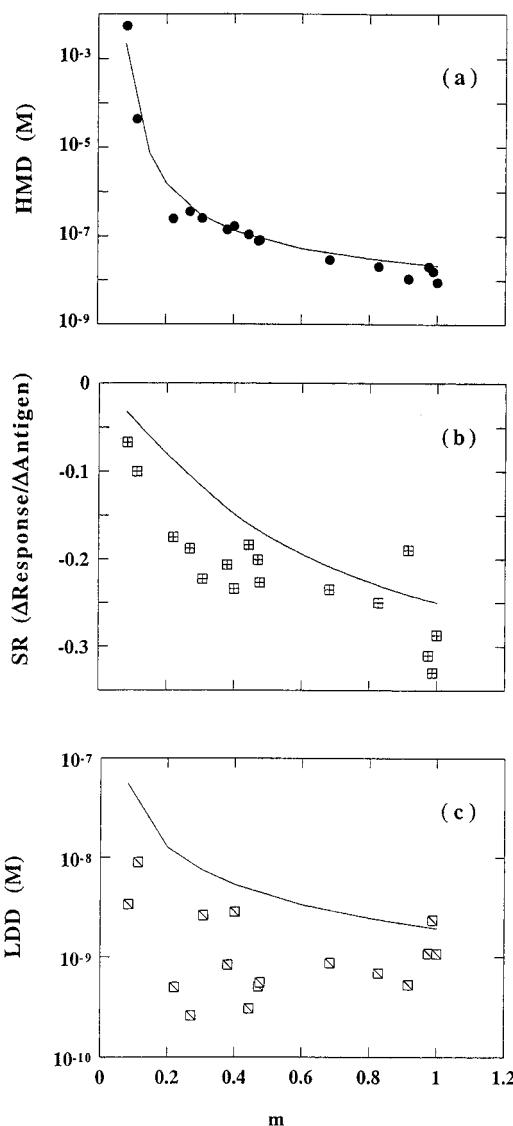


**Figure 6.** Assay performance criteria as predicted by the LLCAM (solid lines) and experiment (open circles) as a function of  $m$  value: (a) half-maximal dose; (b) slope of the response; (c) Least detectable dose.

coverages. Experimental  $m$  values and theoretical  $A/A_0$  values calculated for various values of the percent active antibody as a function of the total antibody surface density are shown in Figure 5. The  $A/A_0$  values were calculated by assuming the percentage of active antibody to determine the area per active site and dividing by the vesicle projected area. Since 0.1 mol % HBVs had a mean diameter of 1480 Å while [ $^{14}\text{C}$ ]HBVs had a mean diameter of 890 Å, two sets of theoretical  $A/A_0$  curves are presented in Figure 5. Curves for 0.1 mol % HBVs (solid lines) at 1%, 2%, and 5% active antibody and a curve for [ $^{14}\text{C}$ ]HBVs (dashed line) at 8% active antibody are compared to experimental  $m$  values for 0.1 mol % HBVs (filled circles) and for [ $^{14}\text{C}$ ]HBVs (open circles). For 0.1 mol % HBVs, the percent active antibody was approximately 5% at 290 ng/cm<sup>2</sup> and decreased to approximately 1% at 50 ng/cm<sup>2</sup>, which is in reasonable agreement with the expected ABA activity of between 20% and 1%. Experimental  $m$  values for [ $^{14}\text{C}$ ]HBVs agreed with theoretical  $A/A_0$  values when a percent active antibody of 8% was used to determine the  $A/A_0$  curve. Over the experimental vesicle size range (1000–1500 Å), the  $m$  values decreased monotonically as the antibody surface density increased, and the  $m$  values obtained for [ $^{14}\text{C}$ ]HBVs agreed with the  $m$  values for 0.1 mol % HBVs.

This indicates that, over this size range, the vesicles are adsorbing with comparable occupied areas.

The LLCAM was used to determine three competitive assay performance criteria: the least detectable dose (LDD), the slope of the response (SR), and the half-maximal dose (HMD). Theoretical values of the performance criteria are compared to experimental values reported earlier (Jones et al., 1994) as a function of the  $m$  value in Figure 6. In Figure 6a, the experimental HMD values (open circles) agree well with predicted values, while in Figure 6b the experimental SR values (open circles) fall just below the theoretical SR values. This demonstrates reasonable agreement between experimental results and theoretical predictions. In Figure 6c, the experimental LDD values are slightly lower than the model predictions. This is because the initial competitive assay response at low biotin concentrations tends to fall below the theoretical prediction, resulting in a lower experimental LDD value.

### Conclusions

Two competitive assay models were presented to describe the competition between a small ligand and either a small or large labeled ligand. The association constants used in the models were obtained from adsorption isotherm measurements. The models agreed with assay data over the range of experimental conditions used. The LLCAM was developed to explain the performance of large multivalent ligands competing with a small univalent ligand for surface binding sites. The results indicated that multiple point attachment of vesicles to the surface can decrease the effectiveness of liposome-based competitive assays and that an optimum surface density of antibodies should be chosen in developing such assays. This model might also be useful in explaining other biochemical recognition phenomena, such as specific cell adhesion and binding of large particles to receptors.

### Notation

[A]	unlabeled analyte concentration in bulk solution
[A*]	labeled analyte concentration in bulk solution
$A$	area per active antibody site
$A_0$	cross-sectional area of a vesicle
DMPE	dimyristoylphosphatidylethanolamine
$h$	heterogeneity index from the Sips equation
HMD	half-maximal dose (see Jones et al., 1994)
$K_0$	average association constant from the Sips equation
$K_1$	association constant for free biotin
$K_2$	association constant for B-HRP
$K_3$	association constant for HBVs
LDD	least detectable dose (see Jones et al., 1994)
LLCAM	large ligand competitive assay model (eq 10)
$m$	adjustable geometrical parameter (eqs 8–10)
$N(K)$	distribution function of binding association constants as given by the Sips equation (eq 4)
$P(\theta)$	probability of the adsorption surface having a binding site large enough to accommodate a large ligand, such as a vesicle, as a function of fractional surface coverage $q$

$S$	specific signal ( $S_{\text{ABA}} - S_{\text{cas}}$ ; see Jones et al., 1994)
$\bar{S}$	average specific signal as computed from the Sips equation (eq 3)
SLCAM	small ligand competitive assay model (eq 1)
$S_0$	specific signal for HBVs or B-HRP measured in competitive assays at low biotin concentrations during competitive assays
SR	slope of the competitive assay response curve (see Jones et al., 1994)

### Greek Letters

$\Gamma_{\text{AB}}$	surface density of unlabeled analyte adsorbed onto active antibody
$\Gamma_{\text{A}^*\text{B}}$	surface density of labeled analyte adsorbed onto active antibody
$\Gamma_0$	surface density of active antibody
$\theta$	fractional surface coverage of vesicles
$\theta_0$	fractional surface coverage of vesicles in the absence of free analyte

### Acknowledgment

The authors gratefully acknowledge the North Carolina Biotechnology Center, the National Science Foundation (BCS-9223193), and AKZO Corporate Research America, Inc., for financial support of this work.

### Literature Cited

- Cecil, R.; Ogston, A. G. Determination of sedimentation and diffusion constants of horseradish peroxidase. *Biochem. J.* **1951**, *49*, 105–106.
- Goding, J. W. *Monoclonal Antibodies: Principles and Practice*, 2nd ed.; Academic Press: London, 1986; p 13.
- Jones, M. A. Ph.D. Thesis, Department of Chemical Engineering, North Carolina State University, Raleigh, NC, 1993.
- Jones, M. A.; Kilpatrick, P. K.; Carbonell, R. G. Preparation and characterization of bifunctional unilamellar vesicles for enhanced immunosorbent assays. *Biotechnol. Prog.* **1993**, *9*, 242–258.
- Jones, M. A.; Kilpatrick, P. K.; Carbonell, R. G. Competitive immunosorbent assay for biotin using bifunctional unilamellar vesicles. *Biotechnol. Prog.* **1994**, *10*, 174–186.
- Nisonoff, A.; Pressman, D. Heterogeneity and average combining constants of antibodies from individual rabbits. *J. Immunol.* **1957**, *80*, 417–428.
- Pauling, L.; Pressman, D.; Grossberg, A. L. The serological properties of simple substances VII. A quantitative theory of the inhibition by haptens of the precipitation of heterogeneous antisera with antigens, and comparison with experimental results for polyhaptenic simple substances and for azoproteins. *J. Am. Chem. Soc.* **1944**, *66*, 784–792.
- Schaff, P.; Talbot, J. Surface exclusion effects in adsorption processes. *J. Chem. Phys.* **1989**, *91*, 4401–4409.
- Sips, R. On the structure of a catalyst surface. *J. Chem. Phys.* **1948**, *16*, 490–495.
- Stankowski, S. Large-ligand adsorption to membranes II. Disk-like ligands and shape dependence at low saturation. *Biochim. Biophys. Acta* **1983**, *735*, 352–360.

Accepted April 22, 1996.®

BP960035W